ChemSusChem

Research Article
doi.org/10.1002/cssc.202300803

Chemistry Europe
European Chemical Societies Publishing

www.chemsuschem.org

Phospholipase D Immobilization on Lignin Nanoparticles for Enzymatic Transformation of Phospholipids

Letizia Anna Maria Rossato,*[a] Mohammad Morsali,[b, c] Eleonora Ruffini,[a] Pietro Bertuzzi,[a] Stefano Serra,[d] Paola D'Arrigo,[a, d] and Mika Sipponen*[b, c]

Lignin nanoparticles (LNPs) are promising components for various materials, given their controllable particle size and spherical shape. However, their origin from supramolecular aggregation has limited the applicability of LNPs as recoverable templates for immobilization of enzymes. In this study, we show that stabilized LNPs are highly promising for the immobilization of phospholipase D (PLD), the enzyme involved in the biocatalytic production of high-value polar head modified phospholipids of commercial interest, phosphatidylglycerol, phosphatidylserine and phosphatidylethanolamine. Starting from hydroxymethylated lignin, LNPs were prepared and successively hydrothermally treated to obtain c-HLNPs with high resistance to organic solvents and a wide range of pH values, covering the conditions for enzymatic reactions and enzyme recovery. The immobilization of PLD on c-HLNPs (PLD-c-HLNPs) was achieved through direct adsorption. We then successfully exploited this new enzymatic preparation in the preparation of pure polar head modified phospholipids with high yields (60–90%). Furthermore, the high stability of PLD-c-HLNPs allows recycling for a number of reactions with appreciable maintenance of its catalytic activity. Thus, PLD-c-HLNPs can be regarded as a new, chemically stable, recyclable and user-friendly biocatalyst, based on a biobased inexpensive scaffold, to be employed in sustainable chemical processes for synthesis of value-added phospholipids.

Introduction

Phospholipids, in addition to being the main components of all biological membranes, are the subject of many areas of biomedical research due to their involvement in critical cellular functions, such as cellular regeneration and differentiation, in addition to their ability to promote the biological activity of various membrane-linked proteins and receptors.[1] Phospholipids have been successfully employed as therapeutic agents, drug-delivery systems, and diagnostic markers for certain diseases.[2] Furthermore, their role in some neurological pathologies such as stress-related disorders, schizophrenia, dementia and Parkinson's disease has been established as well as the beneficial effects of their use in the diet to prevent a range of diseases including inflammation, cancer, and coronary heart issues.[3] Phospholipids are also industrially exploited as natural emulsifiers, surfactants, nutraceuticals, food stabilizers and detergents.[4] Additionally, in the last three years following the onset of the Covid-19 pandemic, phospholipids have been integrated into the design of modern vaccines as liposomal encapsulation systems.[5] Moreover, these residues have also been inserted in biocompatible polymers for medical use.[6]

From a structural point of view, natural phospholipids present a glycerol backbone, esterified at *sn*-1 and *sn*-2 positions with saturated and unsaturated long chain fatty acids, which constitute the lipophilic moieties, and in *sn*-3 with a phosphate diester as the polar head group (see Scheme 1 for abundant natural compounds)

The possibility to prepare different polar head modified phospholipids constitutes a central point in the research on phospholipids because their biological activity is strictly dependent on the chemical identity of the polar head and the acyl chains, and their commercial values are highly related to the source and the purity of the products. However, the preparation of these products is challenging. In fact, even if phosphatidylcholine (PC), which is the most abundant natural phospholipid, is easily extracted from natural sources, the recovery of the other less abundant derivatives is not feasible on a large production scale; it would in fact be extremely expensive, requiring multiple steps of solvent partitioning and chromatography. Obviously, total chemical synthesis from

[a] L. A. M. Rossato, E. Ruffini, P. Bertuzzi, Prof. Dr. P. D'Arrigo
Department of Chemistry, Materials and Chemical Engineering "Giulio Natta"
Politecnico di Milano
piazza L. da Vinci 32, Milano, 20133, Milan (Italy)
E-mail: letiziaanna.rossato@polimi.it

[b] M. Morsali, Prof. Dr. M. Sipponen
Department of Materials and Environmental Chemistry
Stockholm University
Svante Arrhenius väg 16C, SE-10691 Stockholm (Sweden)
E-mail: mika.sipponen@mmk.su.se

[c] M. Morsali, Prof. Dr. M. Sipponen
Wallenberg Wood Science Center,
Department of Materials and Environmental Chemistry
Stockholm University, SE-10691 Stockholm (Sweden)

[d] Dr. S. Serra, Prof. Dr. P. D'Arrigo
Instituto di Scienze e Tecnologie Chimiche "Giulio Natta"
Consiglio Nazionale delle Ricerche (SCITEC-CNR)
via Luigi Mancinelli 7, Milano, 20131 (Italy)

Supporting information for this article is available on the WWW under https://doi.org/10.1002/cssc.202300803

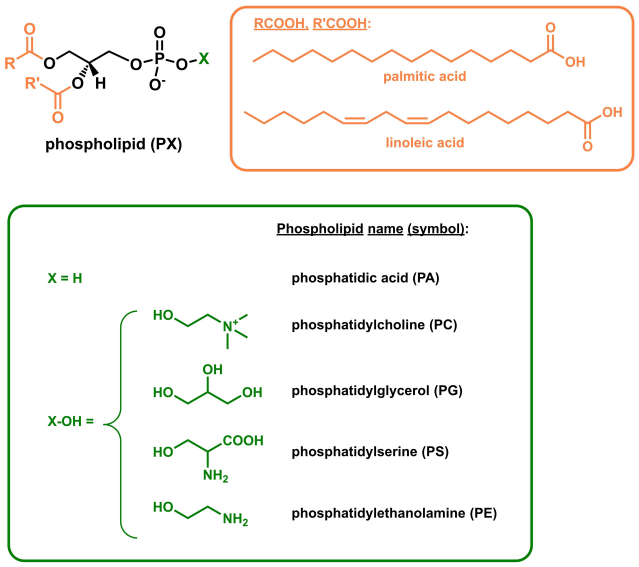

Scheme 1. Structure of the main natural phospholipids. The acyl chains in orange are the most abundant in phospholipids extracted from soybeans.

appropriate homochiral precursors could be exploited but it requires multistep and expensive reagents and the use of complex sequences of protection and deprotection steps in order to introduce selectively the desired functional groups.[7] For that reason, new strategies for the production of these high value compounds are highly desirable.[8] In this context, biocatalytic production starting from natural compounds is a suitable alternative, especially when the final products are required for food and pharmaceutical sectors with strict safety standards. In particular, PC can be enzymatically modified in its polar head moiety into high value phospholipids by means of phospholipase D (PLD, EC 3.1.4.4).[9] This enzyme, in addition to its natural capacity to hydrolyze PC into phosphatidic acid (PA), catalyzes, under definite conditions, the transphosphatidylation reaction of PC in the presence of an alcohol (X-OH), leading to a polar head modified phospholipid reported as PX in Scheme 2.[10]

The reaction parameters could be set in order to reduce the entity of the PA formation which constitutes the parasitic reaction in the preparation of PXs. Some improvements of this strategy were recently reported using novel eco-friendly solvents such as ionic liquids (ILs),[11] deep eutectic solvents (DESs),[10b] and bio-based solvents.[12] PLD is very expensive and not commercially available on large scale as only a few chemical companies produce this enzyme limiting its application to an internal use. For those reasons, the development of enzymatic

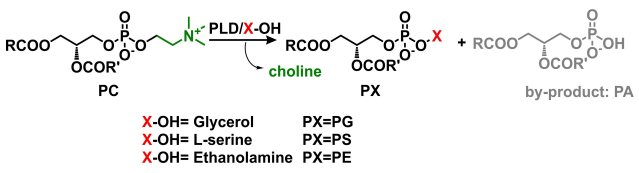

Scheme 2. PLD-catalyzed transformation of PC in polar head modified phospholipids (PXs).

synthesis strategies is highly suitable, particularly when the products are intended for biomedical investigations. In this mainframe, our research has focused on immobilization of PLD, aiming to find new sustainable methods to prepare polar head-modified phospholipids, with the final objective of reducing the operational costs by optimizing the process, recycling the enzyme, and enhancing its activity and stability over time.

In recent years, bio-based enzyme immobilization scaffolds have been highly required to make the industry more sustainable.[13] For that reason, among the components of renewable biomass, a great research interest has grown on lignin, which is an amorphous aromatic polymer constituting the natural glue responsible for structural integrity of plants.[14] Lignin is obtained as a by-product of the pulp and paper industry in which around 70 million tons of lignin are extracted from wood every year. Recently, lignin has become the subject of a wide range of increasingly active research,[15] and particularly spherical lignin nanoparticles (LNPs)[16] with controllable size, desired shape, and high surface area have broadened the window of applications for lignin.[17] LNPs can be prepared using several methods such as pH shifting precipitation,[18] mechanical treatment,[19] sonication[18a,20] and solvent exchange.[21] The solvent exchange method allows preparation of LNPs of controllable size by dissolving lignin in an organic solvent followed by decreasing the organic solvent concentration, commonly by adding water, which initiates aggregation of lignin in a way that results in a colloidally stable dispersion. LNPs have been studied for a plethora of different materials chemistry applications, including drug carriers,[22] UV protectants,[23] and hosts for enzyme immobilization,[24] replacing often hazardous nanomaterials.[25] Our interest in using LNPs for immobilization of PLD was inspired by some recent publications with redox enzymes.[24,26] For example, Capecchi *et al.* described LNPs for the immobilization of tyrosinase for the synthesis of catechol derivatives,[24] and glucose oxidase and peroxidase immobilization to obtain biosensors for the detection of glucose.[26c] In literature, PLD has been immobilized on different supports, such as resins,[27] magnetic nanoparticles,[28] and porous materials,[29] while LNPs appear novel in this domain. We decided to use this kind of scaffold because preparing LNPs is simple, cost-effective and allows the preparation of stable material starting from a largely underutilized bioresource.

However, one of the obstacles limiting widespread use of LNPs in enzyme immobilization has been their instability (aggregation or dissolution) in aqueous and organic solvents. Maintaining the spherical shape and colloidal stability of LNPs is essential not only for the success of the biocatalytic reaction, but also for the extraction processes employed in the products separation o and for the subsequent reuse of the catalyst.

In this work, we present the successful immobilization of PLD on stabilized LNPs obtained from hydroxymethylated lignin by direct adsorption without use of any crosslinkers. The immobilized PLD was studied with particular attention paid to enzyme recycling in the biotransformation of PC in three natural high-value polar head modified phospholipids (as illustrated in Scheme 2): phosphatidylglycerol (PG), phosphati-

dylserine (PS) and phosphatidylethanolamine (PE). These phospholipids were selected for their commercial value due to their peculiar properties. The first product, PG, present in mammalian membranes in a small percentage (1–2% of the total phospholipids),[30] is highly prevalent in mammalian lungs and its concentration in amniotic fluid is used to evaluate the fetal lung maturity and assess the risk of respiratory distress syndrome in new-borns. Therefore, new surfactant preparations based on PG derivatives for therapeutic treatments of this disease are highly requested. The second compound, PS, localized especially in the brain, presents many nutritional and medical functions being involved in many neurological processes.[31] PS has been linked to positive benefits in terms of mind and memory enhancement: in particular it reduces age-related decline in mental function, it prevents Alzheimer's and dementia, it is considered a stress reducer and a mood enhancer to cure depression, and it improves athletic performance. Finally the third product PE is interesting owing to its association with Alzheimer, Parkinson and non-alcoholic liver diseases, as well as with the virulence of certain pathogenic organisms.[32] Moreover, PE could provide beneficial effects to human health because it presents good antioxidant activity against free radicals and has a significant influence on the heart to prevent cell damage.[33]

The present results indicate that stabilized LNPs effectively adsorb PLD and allow efficient biocatalytic transformation of natural phosphatidylcholine into the aforementioned target products. Overall, they constitute a safe and biodegradable material readily prepared from lignin, which is an inexpensive commodity. Thus, PLD-immobilized on these LNPs can be regarded as a new, chemically stable, recyclable and user-friendly biocatalyst to be employed in sustainable chemical processes for phospholipids preparation.

Results and Discussion

Lignin hydroxymethylation

Our work started with the preparation of stabilized lignin nanoparticles (LNPs) for enzyme immobilization. A commercially available and previously fully characterized wheat straw/Sarkanda grass lignin (Protobind 1000)[34] was used as the starting raw material for the preparation of stabilized cured HLNPs (c-HLNPs) as depicted in Figure 1.

In the first step, formaldehyde reacted with lignin at the position 5 of the aromatic ring in an alkaline medium, but some side reaction such as Tollens and Cannizzaro reactions and condensation could also take place (reported in Figure S1). For these reasons, several parameters had to be considered: lignin structure, reaction time and temperature. First, it is known that the hydroxymethylation reaction is strongly dependent on the lignin skeleton, in particular its aromatic ring substitution. In fact, because of its heterogeneous and complex structure, lignin has a low reactivity, and the reactive sites are not available in all aromatic rings.[35] Also, the hydroxymethylation is strongly dependent on the temperature and time of reaction, since undesired condensation reactions could take place at higher temperature and longer time. In our study, the successful hydroxymethylation of lignin was confirmed by FT-IR spectroscopy. The IR spectra showed a broad band absorption in the region of 3400–3200 cm^{-1} which was related to the stretching vibrations of the aliphatic and phenolic O–H groups. The elevated absorbance of the broad band centered at 3350 cm^{-1} in the spectrum of hydroxymethylated lignin (HL) was therefore assigned to increased hydroxyl content (Figure 2a). The increase also of the signals in the region of 3050–2800 cm^{-1} associated with the C–H bonding stretching in the methyl and methylene groups was diagnostic to the hydroxymethylation reaction. Moreover, the lignin modification was notable by the decrease of the signal at 1112 cm^{-1} corresponding to the presence of guaiacyl-syringyl units, the change at 1452 cm^{-1} typical of C–H deformations of asymmetric methyl and methylene, and the appearance of a shoulder at 1290 cm^{-1} corresponding to the increase in guaiacyl units.[36] The hydroxymethylation was also

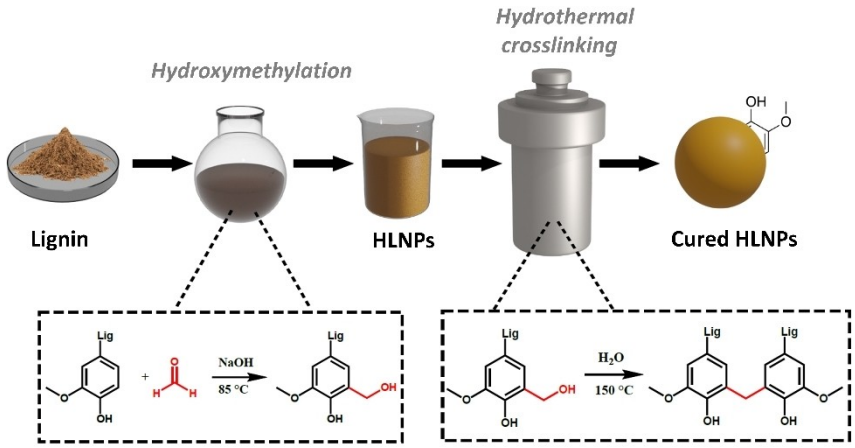

Figure 1. Illustration of the process for the preparation of stabilized c-HLNPs through a hydrothermal curing process.

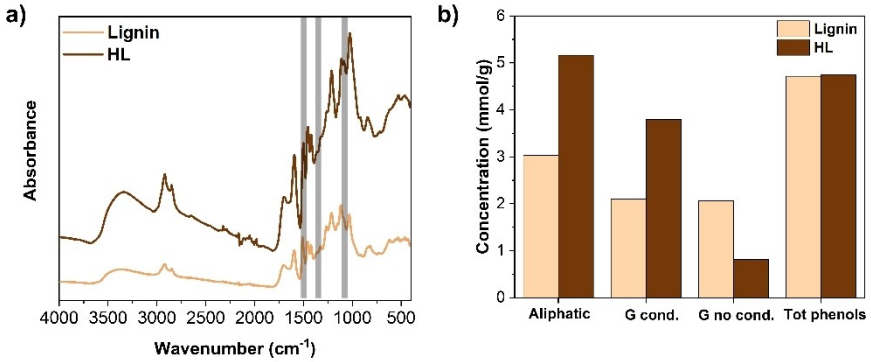

Figure 2. Chemical characterization of LNPs and HLNPs. (a) FT-IR spectra of lignin (in light brown) and hydroxymethylated lignin (HL, in brown). (b) Results of quantitative hydroxyl analysis by ^{31}P NMR spectroscopy of lignin (in light brown) and hydroxymethylated lignin (HL, in brown); cond = condensed.

confirmed by the ^{31}P NMR results (all spectra reported in Figure S2), as shown in Figure 2b by the increase in the aliphatic hydroxyl content of the hydroxymethylated lignin, and the increase and decrease in the G units with substituted and vacant 5-positions, respectively.

Preparation of HLNPs from hydroxymethylated lignin

After dissolution of hydroxymethylated lignin in a mixture of acetone/water 3/1, HLNPs were prepared by precipitation with the addition of deionized water. After filtration to remove possible aggregates, the recovered HLNPs displayed smaller particle size compared to the regular LNPs (Figure 3a). This observation is consistent with the previous literature based only on Kraft lignin.[37] In particular, the size of the LNPs from this kind of lignin is known to decrease with the increasing aliphatic hydroxyl content, and it is also confirmed for LNPs from Protobind lignin, which is a lignin with different chemical and physical properties compared to those of Kraft lignin.

To increase resistance of HLNPs to organic solvents and to a wide range of pH values we aimed to stabilize the HLNPs via intraparticle curing (see Figure 1). So, the resistance of HLNPs and their cured counterparts (c-HLNPs) to withstand a shift from pH 5 to pH 10 (selected range further investigated in PLD activity assays) was tested with DLS analysis, by monitoring their dimensions and polydispersity (PDI) during a 24 h time period after the addition of an aqueous pH 10 buffer. As reported in Figure 4a, c-HLNPs showed a high stability over time in a pH range from 5 to 10, with stable size and PDI. In contrast, uncured HLNPs were rapidly disrupted at pH 10, leading to an irregular size distribution and a high PDI (Figure 4b). This was also visible in the images included in the two graphs: c-HLNPs at basic pH could be recovered by precipitation, while the uncured ones immediately disaggregated probably due to their extensive dissolution. Moreover, in addition to alkaline stability, c-HLNPs appeared stable in organic solvents, such as ethanol, acetone, hexane and toluene. This is a crucial factor for their application in biocatalysis, in particular in enzymatic transformations of phospholipids, since the reactions took place in a biphasic environment (organic solvent-buffer solution). The morphology of the c-HLNPs recovered after incubation at basic pH for 24 h was also analyzed by SEM, showing spherical and intact colloidal particles (see Figure 4c).

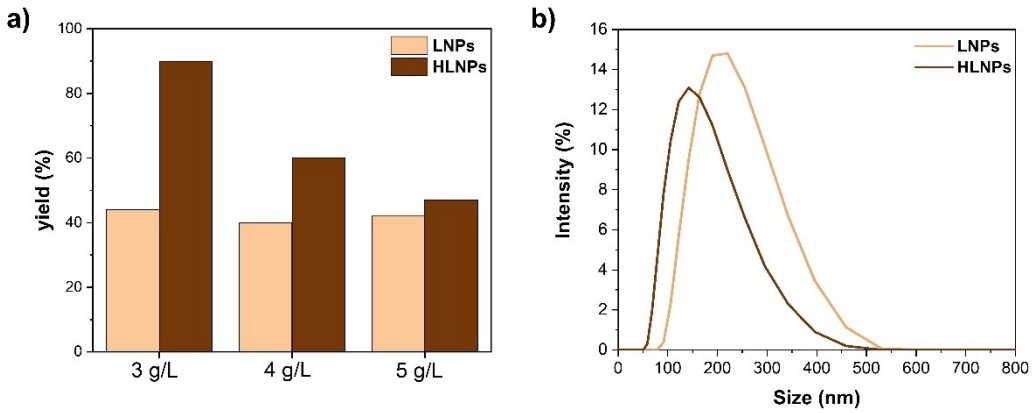

Figure 3. (a) Yields of nanoparticles formation at different lignin concentrations (3, 4 and 5 g/L) for the preparation of LNPs (in light brown) and HLNPs (in brown). (b) Particle size distribution (DLS) of LNPs (in light brown) and HLNPs (in brown) at 3 g/L.

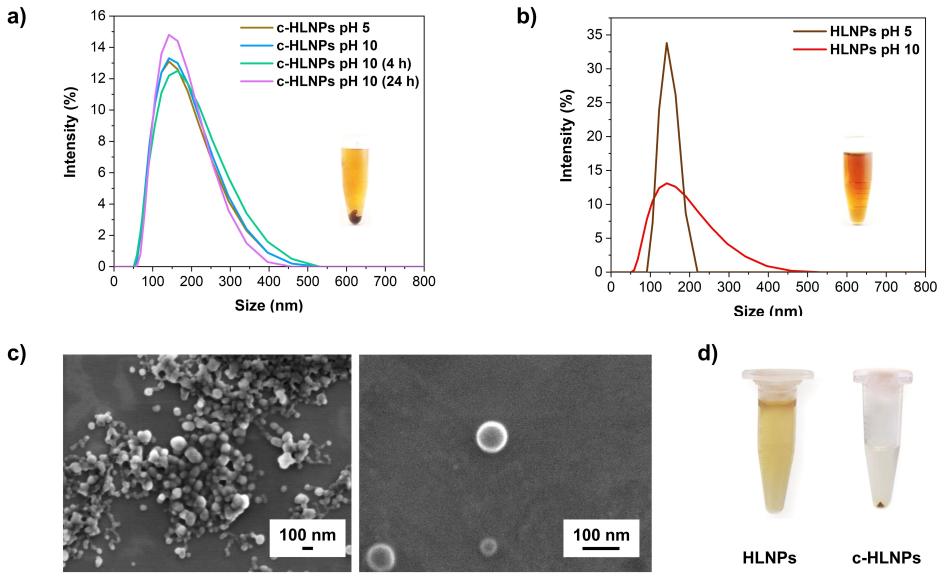

Figure 4. Stability analysis of HLNPs and c-HLNPs. (a) Kinetic of stability for c-HLNPs at pH 10 over 24 h in comparison of the HLNPs at pH 5 (the inset picture shows the appearance of c-HLNPs at pH 10 after centrifugation). (b) DLS analysis of HLNPs (not cured) at pH 5 and at pH 10 (the inset picture shows the appearance of HLNPs at pH 10 after centrifugation). (c) SEM image of c-HLNPs at pH 10 (the scale bars correspond to 100 nm). (d) Photographs of acetone suspension of HLNPs and c-HLNPs after centrifugation.

Phospholipase D immobilization

Phospholipase D activity

The PLD activity was measured from the fermentation broth (PLD_B), the dialyzed broth (PLD_D) and the freeze-dried preparation (PLD_{DL}) and the results are reported in Table 1. The enzyme obtained post-dialysis (PLD_D) showed a higher activity than the broth itself, due to the performed enzyme precipitation (0.3 vs 0.14 U/mL). However, if we compare the immobilized enzymes, PLD_D-c-HLNPs showed an activity almost equal to the PLD_B-c-HLNPs, probably because a plateau in enzyme immobilization capacity on the c-HLNPs was reached. A confirmation of the occurred immobilization was also given by the measurement of the activity of the supernatants sampled after the enzyme had been immobilized on c-HLNPs. In fact, the PLD_B activity of the supernatant was 0.08 U/mL and 0.04 U/mL for PLD_D-c-HLNPs, i.e., only 25% and 13% of the corresponding total activities assayed in the supernatant and pellet fractions. It should be pointed out that the supernatants could contain smaller lignin nanoparticles which could be responsible of residual enzymatic activity into these fractions. Furthermore, the immobilized lyophilized PLD (PLD_{DL}-c-HLNPs) showed an activity of 0.43 U/mL, much higher than the immobilized PLD_B/PLD_D, thanks to the enzyme concentration step. For PLD_{DL}-c-HLNPs the low residual activity of the recovered supernatant after immobilization (0.04 U/mL) was consistent with the results obtained for PLD_B and PLD_D immobilization, and attested that PLD tended to adsorb on c-HLNPs.

The increase in PLD activity after immobilization likely originates from conformational changes once it is adsorbed on LNPs surface. In fact, as reported in literature, the immobilized enzyme loses its flexibility and its 3D structure becomes rigid in the hyperactivated form.[38] The immobilization was also confirmed by the FT-IR analysis (Figure 5a), since the spectrum for free PLD_{DL} (reported in light green) and PLD_{DL}-c-HLNPs (dark green) both showed several diagnostic peaks. In particular, there are four main characteristic signals: (i) CONH peptide linkage at 1650 cm^{-1}; (ii) the presence of COC groups at 1100 cm^{-1}; (iii) NH bending signal for amine I in the area between 1650 and 1580 cm^{-1}; and (iv) CN stretching typical for aliphatic amine between 1250 and 1020 cm^{-1}. Moreover, the

Table 1. Comparison of the PLD activity in free enzyme preparations and in their immobilized forms on c-HLNPs (fermentation broth (PLD_B), immobilized fermentation broth (PLD_B-c-HLNPs), broth post dialysis (PLD_D) and immobilized broth post dialysis (PLD_D-c-HLNPs), lyophilized PLD (PLD_{DL}) and immobilized lyophilized PLD (PLD_{DL}-c-HLNPs)).

Free enzyme			Immobilized enzyme on c-HLNPs (PLD_X-c-HLNPs)			
Composition	Acronym	Activity	Acronym	Activity	Supernatant activity	Retained activity
Fermentation broth	PLD_B	0.14 U/mL	PLD_B-c-HLNPs	0.26 U/mL	0.08 U/mL	75%
Dialyzed broth	PLD_D	0.30 U/mL	PLD_D-c-HLNPs	0.23 U/mL	0.04 U/mL	87%
Lyophilized enzyme	PLD_{DL}	0.026 U/mg	PLD_{DL}-c-HLNPs	0.43 U/mL	0.04 U/mL	91%

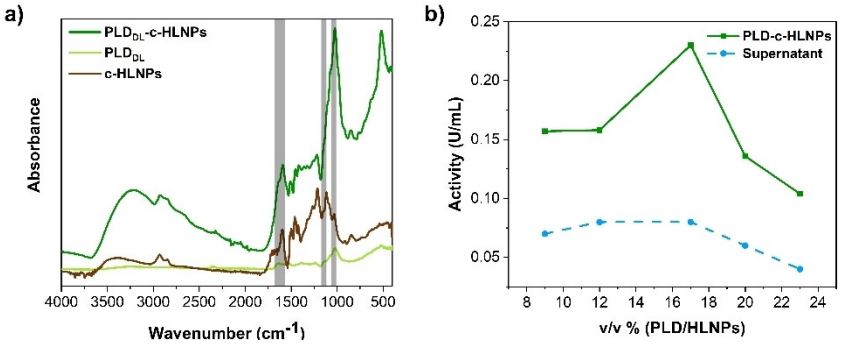

Figure 5. (a) FT-IR spectra of PLD_{DL} (in light green), c-HLNPs (in brown) and PLD_{DL}-c-HLNPs (in dark green); (b) Activity (U/mL) of PLD-c-HLNPs (in dark green) and supernatant (in blue) obtained after enzyme immobilization.

DLS size distribution showed that the immobilization increased the particle diameter compared to the original HLNPs (c-HLNPs: 120 nm; PLD_{DL}-c-HLNPs: 200 nm).

Concentration effect

The effect of the enzyme concentration was tested to determine the best condition in which almost all the enzyme could be immobilized without losing activity. We tested several different enzyme concentrations in lignin particle dispersions: 9%, 12%, 17%, 20% and 23% v/v (PLD/HLNPs suspension). The results showed that, when the 17% v/v of PLD (equivalent to 48 μg PLDDL/g c-HLNPs and to 1.18% PLDDL/lignin w/w) was immobilized, a plateau was reached and the addition of more enzyme provoked a decrease in the recovered activity (Figure 5b). Most likely, after the level of 17% v/v, all the surfaces of c-HLNPs were covered, and the enzyme started to form multilayers, covering the active site of the enzyme underneath, and causing a decrease in the activity. By increasing the concentration of PLD, also the activity of the supernatant decreased proving that the enzyme was almost completely immobilized (Figure 5b).

Temperature and pH effect

Temperature and pH were tested to select the best parameters for the biocatalytic transformations. The temperature dependence of the enzymatic activity on PC was assayed in the 10–70 °C range at pH 8. As reported in Figure 6a, PLD-c-HLNPs showed the highest activity at 40 °C. Though the temperature optimum was similar to that of the free PLD, the immobilized enzyme was markedly more active, with almost two-fold activity in comparison to the value obtained for the free enzyme. Concerning the influence of pH on enzymatic activity, PLD-c-HLNPs tested in the 2–13 pH range appeared to be more active at pH 4 whereas the free enzyme was more active at pH 6 (Figure 6b). Also, in this case, the PLD-c-HLNPs were markedly more active than the free enzyme across the pH range. The increase in PLD activity after immobilization even when it is submitted to not-optimal conditions of temperature and pH is due to the fact that the enzyme conformation, once it is immobilized, remains stable, loses the flexibility, overcomes its fragile nature, and even tolerates extreme reaction environments such as harsh pH and temperatures.

These results are particularly interesting since the trans-phosphatidylation reactions reported in this paper are performed at 40 °C and at pH 5.6 (phosphatidylglycerol and phosphatidylethanolamine) and 4.5 (phosphatidylserine). As shown in Figure 6, PLD-c-HLNPs activity is particularly higher under these conditions, and even higher than that of the free

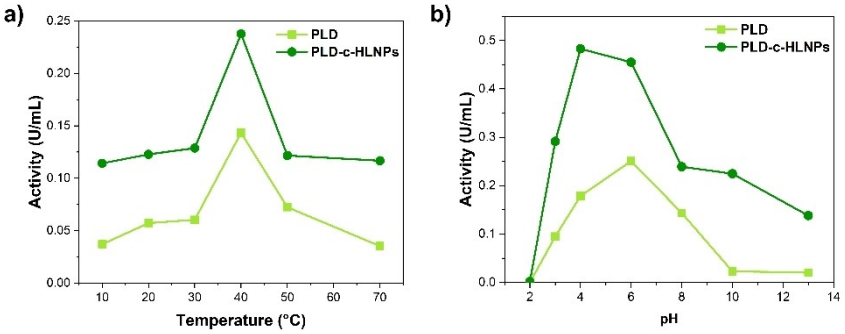

Figure 6. (a) Activity (U/mL) of PLD and PLD-c-HLNPs in a range of temperatures between 10 to 70 °C; (b) Activity (U/mL) of PLD and PLD-c-HLNPs in a pH range from 2 to 13 at 40 °C.

enzyme, making phosphatidylcholine transphosphatidylation particularly advantageous.

Enzymatic synthesis of polar head modified phospholipids

Our ultimate objective in the present work was to study the possibility to exploit the immobilized PLD on c-HLNPs in the enzymatic transformation of natural PC, investigating a new protocol for the production of three important polar head modified phospholipids (PXs), namely phosphatidylglycerol (PG), phosphatidylserine (PS) and phosphatidylethanolamine (PE). In these compounds the choline residue of PC is substituted by a glycerol, a L-serine and an ethanolamine moiety respectively (see Scheme 1). For that purpose, purified PC from soya beans was used as substrate. Because of its natural source, the major acyl chain pattern of PC resulted in a mixture of palmitic (C16:0) and linoleic (C18:2) acid chains as previously reported (see Figure S3).[10b] PC and the corresponding alcohols (glycerol, L-serine and ethanolamine) were converted into PXs by PLD_{DL}-c-HLNPs in a biphasic system at 40 °C. At the end of each synthetic cycle, after centrifugation of the reaction mixtures, the final products PXs were easily recovered with high yields that in the case of PG and PS exceeded 90%, while for PE it reached 60% (Figure 7). The final products were analyzed by ESI/MS in order to confirm their high purity and the complete transformation of the starting substrate PC.

The spectra of all the products obtained after four recycling steps are reported in Figure 8 (with PC spectrum for comparison). The supported enzyme preparations were, within each PX preparation, successfully completely recycled with high activity retention over four synthetic cycles (complete ESI/MS spectra are reported in Figures S4, S5, S6 for PG, PS and PE respectively). It is important to underline that this method of enzyme immobilization allowed, compared to the previously cited literature, to recover the desired products in high yields (consistently with our previous works),[39] constantly over the cycles, and that the enzyme activity remained quite unchanged without losing efficiency. Moreover, the immobilized enzyme showed a higher activity with respect to the free one, allowing to reduce the reaction times. These factors make the system suitable for the immobilization and recyclability of the enzyme, paving the way for further investigations for different biocatalytic processes.

Comparison of PLD immobilization on c-HLNPs and other supports

In literature, PLD has been immobilized on different supports, such as magnetic nanoparticles and porous materials. In particular, Li *et al.*[40] immobilized PLD on silicon dioxide nanoparticles using solvent precipitation and glutaraldehyde as cross-linker; Han *et al.*[28] reported the PLD immobilization on silica-coated magnetic nanoparticles only by direct adsorption; finally Li *et al.*[41] synthetized PS by PLD immobilized on an inorganic hierarchical porous material prepared via a template-free approach. All these aforementioned methods resulted in an increased enzyme activity, enhancing its stability over a wide range of temperatures and pH and allowed recycling of the enzyme. In comparison to these works, our technique allows to immobilize PLD on a low-cost, renewable scaffold without the addition of cross-linker, while still increasing the enzyme performance. In fact, the enzyme recovery rate after immobilization was high (> 75%), and PLD increased its activity of almost two times at the optimal pH and temperature. These are positive results when compared to the literature. Li *et al.* reported that the PLD activity increased of 1.15 times due to its

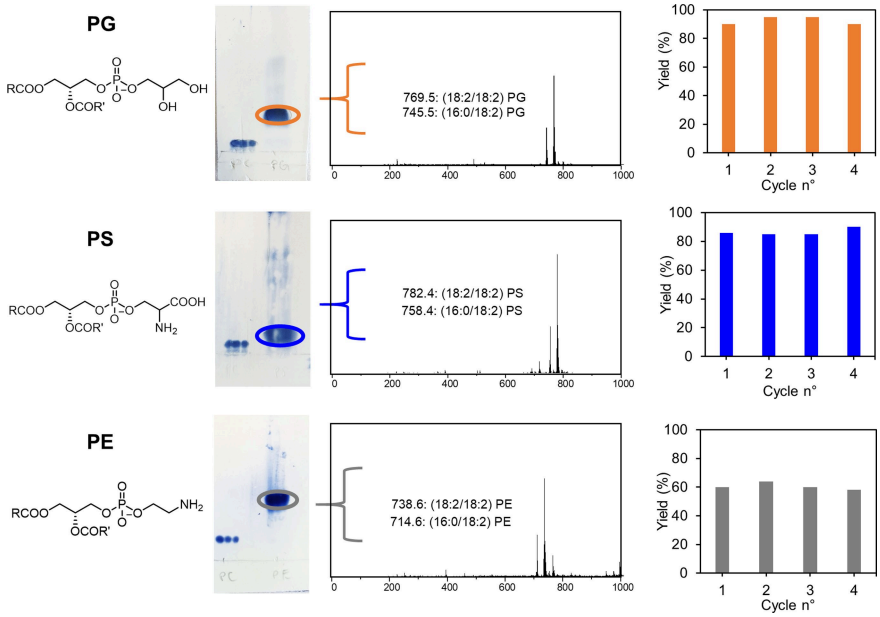

Figure 7. Structure, characterization (TLC and ESI/MS spectra) and yield of production (over 4 cycles) of PG, PS and PE.

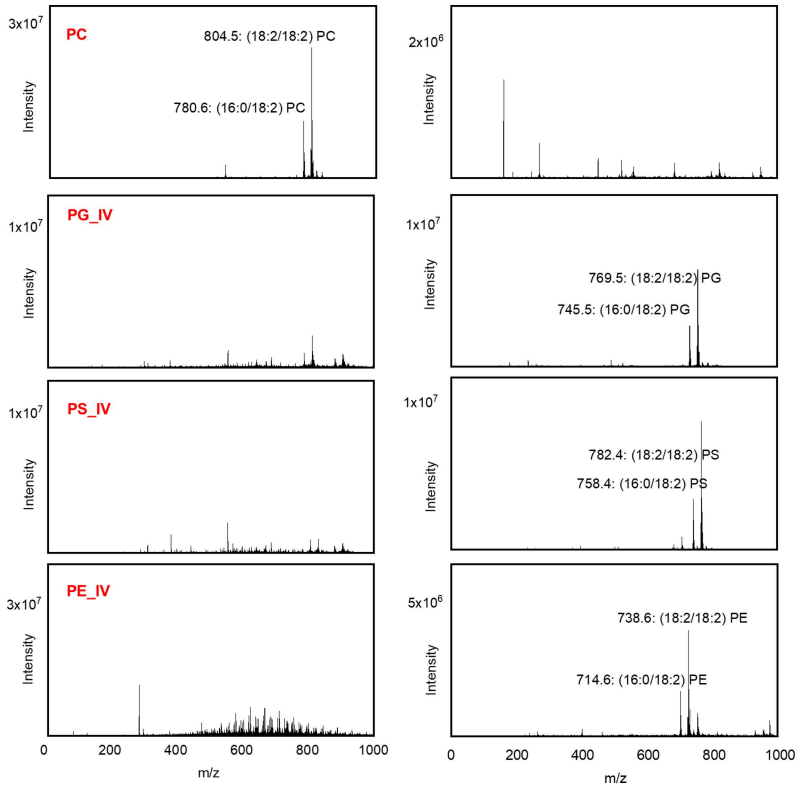

Figure 8. ESI/MS of starting PC and of final PG, PS and PE products obtained with PLD-HLNPs in the fourth step (indicated as PX_IV) of recycling. On the left side the positive ions spectra are reported, on the right side the negative ones.

immobilization on silicon dioxide nanoparticles[40], while in the study of Han *et al.* the PLD activity remained constant at the reaction conditions (40 °C, pH 6.2), and the extent of enzyme recovery was less than 60 %.[28] In these aforementioned studies of Li et al.[40] and Han et al.[28], a notable shift in the optimal temperature and pH occurred, which no longer correspond to the conditions under which the transphosphatidylation reactions are performed. Instead, in the present study the immobilized PLD preserved its optimal reaction conditions, without shifting of temperature, allowing to perform the transphosphatidylation reactions at 40 °C, as previously reported in literature.[42]

Green metrics

This study resonates with the green chemistry principles firstly introduced by P.T. Anastas and J.C. Warner in 1998.[43] In this scenario, we calculated some of these parameters to prove the greenness of this technique. In particular, E- factor (g of waste/g product), Atom Economy (Mw product/Mw reagents), productivity (g product/g enzyme/h) and PMI (kg of raw material/kg of products) have been evaluated for all the three products, and they are reported in the Tables S1-S4. In general, these results show that the reported method produces a low amount of waste and the reaction efficiency is good.

Conclusions

In this work, we immobilized an phospholipase D on a sustainable scaffold which has been exploited in the production of high value polar head modified phospholipids. In particular, biobased stabilized nanoparticles were obtained by the precipitation of an hydroxymethylated technical lignin followed by a successive hydrothermal curing step. These c-HLNPs appeared to be stable in organic solvents and at different pH values and were exploited for the immobilization of the expensive enzyme PLD by a facile adsorption process, without the use of covalent crosslinking reactions. The PLD-c-HLNPs system was exploited for the production of functional phospholipids of high commercial interest, namely phosphatidylglycerol, phosphatidylserine, and phosphatidylethanolamine, showing higher catalytic efficiency than the free PLD. The method allowed the efficient recycling of PLD and high reaction yields (60–90 %), without losing its activity for four cycles. The present work thus constitutes a new sustainable approach for the biocatalytic preparation of polar head modified phospholipids exploiting lignin nanoparticles as a valuable biobased and inexpensive tool for PLD immobilization, paving the way to the exploitation of this procedure in other biocatalytic processes, in particular when expensive enzymes are required.

Experimental section

All chemicals, solvents and enzymes (choline oxidase and peroxidase) were purchased from Merck (Merck Life Science S.r.l., Milan, Italy) and used as received without further purification. Phosphatidylcholine (PC) was supplied from Lucas Meyer (Epikuron 200, soy lecithin) and used after purification by precipitation in cold acetone (10 g of Epikuron 200 dissolved in 15 mL of hexane, added to 300 mL of cold acetone). ^{1}H NMR and ^{31}P NMR spectra were recorded on a 400 MHz Bruker Avance spectrometer (Milano, Italy). Acquisition and data treatment were performed with Bruker TopSpin 3.2 software. Chemical shifts were reported in δ units (ppm), the spectra were recorded in $CDCl_3$/CD_3OD for phospholipids, and a mixture of $CDCl_3$/pyridine for lignin analysis. Deuterated solvents were purchased from Eurisotop (Saint-Aubin, France). Protobind 1000 (a mixed wheat straw/sarkanda grass lignin from soda pulping of non-woody biomass) was purchased from Tanovis (Alpnach, Switzerland) and is referred to as lignin in this work.

PLD preparation

Microrganism fermentation. PLD was obtained from the fermentation broth of *Streptomyces netropsis* (DSM 40093) as reported in our previous works (see Figure S7).[39] The medium for strain growth and maintenance was composed of glucose 4 g/L; yeast extract 5 g/L; malt extract 10 g/L whereas the medium for PLD preparation contained glucose 5 g/L, yeast extract 5 g/L, malt extract 10 g/L, peptone from soybean 3 g/L, peptone from casein 1 g/L, $MgSO_4$ 0.2 g/L, NaCl 0.2 g/L. The fermentation was performed aerobically, setting a minimum air flow of 2 L/min (0.5 v/v/min), in a sterilized fermenter vessel of a 5 L bioreactor (Biostat A BB-8822000, Sartorius Stedim, Göttingen, Germany) containing 4 L of medium. Temperature, stirring speed, and pH were set to 30 °C, 250 rpm and 7.0, respectively. pH value was controlled by addition of sterilized aqueous solutions (10% w/w in water) of either acetic acid or ammonia. After 48 h, the fermentation broth was filtered through a celite pad, and the clear liquid was stored at 4 °C in dark bottles.

Precipitation and dialysis. To 1 L of the filtered broth, 430 g of ammonium sulfate were added over 1 h at 4 °C under stirring. After its dissolution, the broth was left precipitating overnight at 4 °C. After 24 h, the pellet was recovered by centrifugation at 8000 rpm for 15 min at 4 °C. The solid was then dissolved in a small amount of supernatant broth and dialyzed with a seamless cellulose tube (D0655 Sigma-Aldrich, Milano, Italy) against 10 mM sodium acetate buffer at pH 5. The dialyzed broth (100 mL), which had an activity of 0.30 U/mL, was finally lyophilized (0.026 U/mg, see Figure S7 for the scheme of PLD preparation).

Thin Layer Chromatography (TLC)

TLC plates Silica gel 60 SIL G-25 UV254 glass 250 μm (Macherey Nagel) were used for analytical TLC. The eluent was constituted by $CHCl_3$/CH_3OH/CH_3COCH_3/CH_3COOH/H_2O: 50/10/20/10/5 (ratios reported in volume). Detection was performed by staining with cerium molybdate reagent and 0.2% ethanolic ninhydrin solution (TLC reported in Figure S8).

Electrospray Ionization Mass Spectrometry (ESI/MS)

Mass spectra were recorded on an ESI/MS Bruker Esquire 3000 PLUS (ESI Ion Trap LC/MSn System, Bruker, Milano, Italy), by direct infusion of a dichloromethane solution of compounds with an infusion rate of 4 μL/min. Samples were analyzed using both positive and negative ionization modes to allow the detection of all relevant compounds.

Preparation of hydroxymethylated lignin

Hydroxymethylated lignin (HL) was prepared using an existing method as reported in Morsali *et al.*[37b] Briefly, in a round bottom glass, 8.75 mL of deionized water and 11.25 mL of aqueous sodium hydroxide (1 M, 11.25 mmol) were added to 5 g of dry lignin to dissolve lignin at pH 10.5 in room temperature. Then 5 mL of formaldehyde solution (37% formaldehyde, 66 mmol) was added dropwise to the lignin solution and temperature was increased to 85 °C. The reaction was allowed to take place for 4 h. Subsequently, deionized water was used to quench the reaction and the pH was adjusted to 3 with addition of 0.1 M hydrochloric acid drop by drop. The product was centrifuged and washed 3 times with deionized water to remove extra acid and formed salts. The purified product was freeze-dried to collect dry HL.

Preparation of nanoparticles from hydroxymethylated lignin (HLNPs)

HL (430 mg) was dissolved in acetone/water mixture 3/1 (9.37 g/3.12 g) and let stirring 2 h. Then the sample was filtered to remove the impurities, and the LNPs were produced by quickly pouring deionized water (37 mL) to the lignin solution while stirring. Subsequently, acetone was removed by evaporation, and the final aqueous dispersion of HLNPs was obtained by filtration to remove possible aggregates. HLNPs (yield 80%) were diluted to the final concentration of 5 g/L on a total volume of 40 mL. The colloidal dispersion of HLNPs (5 g/L) was hydrothermally cured in a Teflon-sealed reactor at 150 °C overnight to give cured HLNPs (reported as c-HLNPs).

Dynamic Light Scattering (DLS) and Zeta potential

The particle size and zeta potential of HLNPs and PLD-HLNPs were measured using a Zetasizer Nano ZS90 instrument (Malvern Instruments Ltd., UK). Zeta potential was determined using a dip cell probe. Measurements were carried out with three replicates of the particle diameter (Z-average, intensity mean) and zeta potential, and the mean values were used for the study.

Fourier Transform Infrared Spectroscopy (FT-IR)

FT-IR data were collected using a Varian 610-IR FT-IR spectrometer. The IR absorbance of samples was measured using an attenuated total reflection–Fourier transform infrared spectrophotometer (ATR-FTIR) in the 450–4000 cm^{-1} wavenumber range.

Scanning Electron Microscopy (SEM)

SEM imaging was conducted using a JEOL JSM-7401F (JEOL Ltd., Japan) using a secondary electron detector. Samples for imaging were diluted 50 times using deionized water and drop-casted on a silicon wafer.

^{31}P Nuclear Magnetic Resonance Spectroscopy (^{31}P NMR)

Quantitative analysis of hydroxyl groups of lignin and HL was conducted using ^{31}P NMR spectroscopy following the known procedure.[44] Briefly, the samples (30 mg), dissolved in N,N-dimethylformamide, were phosphitylated with 2-chloro-4,4,5,5-tetramethyl-1,3,2-dioxaphospholane (0.9 mmol) in the presence of N-hydroxy-5-norbornene-2,3-dicarboxylic acid imine (0.010 mmol) as an internal standard and chromium(III) acetylacetonate as a relaxation agent. The ^{31}P NMR experiments (256 scans, 10 s

relaxation delay) were performed in $CDCl_3$/pyridine mixture with 90° pulse angle and inverse gated proton decoupling (reported in Figure S2).

For phospholipids analysis, 50 mg of sample were dissolved by vigorous stirring with 5 mg of triphenyl phosphate in 0.6 mL of a $CDCl_3$/CDH_3OD 2/1 solution mixed with 0.4 mL of a CsEDTA solution (prepared by titration of 0.2 M EDTA in D_2O with $CsCO_3$ until pH 7.6, then diluted 1:4 (v/v) with methanol). After complete solubilization, water (0.2 mL) was added and the solution was stirred again. The solution was transferred into an NMR tube and left to rest in order to achieve the correct separation of the two liquid phases. The ^{31}P uncoupled experiments were performed with the following parameters: D1: 10 s, SW: 40 ppm, O1: −10 ppm, FID size: 32768, ns: 32, T: 320 K.

Enzyme immobilization

Fermentation broth immobilization (PLD_B-c-HLNPs). The fermentation broth (PLD_B) was added dropwise to 5 mL of c-HLNPs (5 g/L) suspension under stirring at different concentrations. The mixture was let stirring for 2 h and then centrifuged 3 times at 8000 rpm for 10 min each. The collected supernatant was centrifuged once at 10000 rpm for 15 min to recover the smallest nanoparticles which were then added to the first precipitate and were labelled as PLD_B-c-HLNPs.

Dialysed broth immobilization (PLD_D-c-HLNPs). The concentrated fermentation broth (PLD_D), coming from the dialysis process, was added dropwise to 5 mL of c-HLNPs (5 g/L) suspension under stirring at different concentration. The mixture was stirred for 2 h and then centrifuged 3 times at 8000 rpm×10 min. The collected supernatant was centrifuged once more at 10000 rpm×15 min to recover the smallest nanoparticles which were then added to the first precipitate and were labelled as PLD_D-c-HLNPs.

Lyophilized broth immobilization (PLD_{DL}-c-HLNPs). Lyophilized PLD (PLD_{DL}) was immobilized on c-HLNPs by dissolving the enzyme powder at different concentrations in deionized water. Then 1 mL of the enzyme solution was added dropwise to 5 mL of c-HLNPs (5 g/L) suspension under stirring. The mixture was stirred for 2 h and then centrifuged 3 times at 8000 rpm×10 min. The collected supernatant was centrifuged once at 10000 rpm×15 min to recover the smallest nanoparticles which were then added to the previous precipitate and were labelled as PLD_{DL}-c-HLNPs.

PLD activity determination

The activity was measured following a standard procedure.[45] Briefly 50 mg of PC were dissolved in 2 mL of Triton-X 10% v/v and 2 mL of buffer TRIS 0.1 M pH 8 (indicated as buffer T in the present section). 3 mg/mL of 4-aminoantipyrine and 2 mg/mL of phenol were dissolved in buffer T and then mixed together and diluted with buffer T until a final volume of 14.6 mL was reached (Solution A). Choline oxidase was dissolved in buffer T at final concentration of 50 U/mL, while peroxidase at final concentration of 100 U/mL. A solution of $CaCl_2$ 0.1 M in buffer T was also prepared. For each measurement 134 μL of PC were mixed to 34 μL of $CaCl_2$ solution and 10 μL of enzyme. The sample was left stirring 10 min at 40 °C. Then 700 μL of Solution A, 67 μL of peroxidase and 67 μL of choline oxidase were added. If the enzyme was immobilized on the nanoparticles, the suspension was centrifuged before UV analysis. The analyses were performed at λ of 550 nm for 20 min with a UV-Vis Double Beam Spectrophotometer V-730 Jasco (Jasco Europe, Cremella, Italy). The enzymatic activity was calculated with the expression here below:

$$U/mL = [(\Delta Abs/min \times V_f)/(\varepsilon \times V_e)] \times D$$

where V_f = cuvette total volume (mL); ε = 6 ($M^{-1}\,cm^{-1}$); V_e = enzyme volume (mL); D = dilution factor.

For each experiment, when immobilized PLD and the free enzyme are compared, they have been used in the same amount.

Concentration-activity relationship for PLD-c-HLNPs

The PLD-c-HLNPs system activity was measured by immobilizing different concentrations of enzyme on the c-HLNPs, ranging from 9% to 23% v/v% (PLD/c-HLNPs). The activities of the supernatants were also tested. However, it is important to precise that these last values could be overestimated by the presence of the smallest c-HLNPs which may remain suspended in the supernatants despite the centrifugation steps.

Temperature -activity relationship for PLD-c-HLNPs

The temperature dependence of PLD-c-HLNPs activity was investigated towards PC performing the incubation of the reaction mixture thermostated at temperatures ranging from 10 to 70 °C. Then, after the centrifugation for enzyme recovery, the sample was analysed with the activity test described above.

pH-Activity relationship for PLD-c-HLNPs

The pH dependence of the PLD-c-HLNPs activity towards PC was determined by incubating the reaction mixture using the appropriate 0.1 M buffer for 10 min at 40 °C in the 2–13 range adjusted to the appropriate pH with HCl or NaOH. Then, after the centrifugation for enzyme recovery, the sample was analysed with the activity test described above.

Enzymatic preparation of phosphatidylglycerol (PG)

30 mg of lyophilized PLD (0.026 U/mg) were dissolved in 1 mL of 0.1 M sodium acetate buffer pH 5.6 and 0.1 M of calcium chloride, and added dropwise to 5 mL of c-HLNPs (5 g/L). After 2 h, 8 M glycerol (4.41 g) was added and the solution brought to pH 5.6 by addition of acetic acid. The solution was added to PC (10 mg) preliminary dissolved in 1 mL of toluene. The reaction was left under stirring at 40 °C for 24 h. Then the two phases were separated by centrifugation at 8000 rpm 2 min, and the aqueous phase was extracted twice with toluene (2×5 mL). The organic phases were collected, dried with sodium sulfate and the solvent was evaporated under reduced pressure. The PLD-c-HLNPs system was collected and recycled for 4 cycles, adding for each of them fresh PC. No addition of glycerol was required. The 3rd and the 4th cycles were left under stirring at 40 °C for 30 h and 48 h respectively to obtain the major conversion of the substrate into PG. For each cycle, the product was recovered in a mass yield of 85–90%. ^1H NMR (spectrum reported in Figure S9): 0.75–0.85 (m, 6H, CH_3), 1.15–1.36 (m, 30 H, CH_2 acyl chains), 1.48–1.60 (m, 4H, $\underline{CH_2}$-CH_2-COO), 1.92–2.04 (m, 5 H, $\underline{CH_2}$-CH=CH), 2.18–2.29 (m, 4H, $\underline{CH_2}$-COO), 2.67–2.77 (m, 3H, CH=CH-$\underline{CH_2}$-CH=CH), 3.50–3.66 (m, 2H, CHOH-$\underline{CH_2}$OH), 3.74–4.00 (m, 5H, $\underline{OCH_2}$-CH-$\underline{CH_2}$-OPO_3 and $\underline{CH}$OH-CH_2OH), 4.05–4.15 (m, 1H, OPO_3-CH_2), 4.28–4.38 (m, 1H, OPO_3-$\underline{CH_2}$), 5.10–5.21(m, 1H, OCH_2-$\underline{CH}$-CH_2-OPO_3), 5.23–5.38 (m, 6H, CH=CH). ESI/MS negative ion spectrum (reported in Figure S4): m/z 16:0/18:2-PG $[745.5]^-$, 18:2/18:2-PG $[769.5]^-$. ^{31}P NMR δ: 0.51 ppm.

Enzymatic preparation of phosphatidylserine (PS)

30 mg of lyophilized PLD (0.026 U/mg) were dissolved in 1 mL of 0.1 M sodium acetate buffer pH 4.5 and 0.1 M of calcium chloride, and added dropwise to 5 mL of c-HLNPs (5 g/L). After 2 h, 3 M L-serine was added and the solution brought to pH 4.5 by addition of acetic acid. The solution was added to PC (10 mg) preliminary dissolved in 1 mL of toluene. The reaction was left at 40 °C under stirring for 24 h. Then the two phases were separated by centrifugation at 8000 rpm for 2 min, and the aqueous phase was extracted with toluene (2×5 mL). The organic phases were collected, dried with sodium sulfate and the solvent was evaporated under reduced pressure. The PLD-c-HLNPs system was collected and recycled for 4 cycles, by addition every time of a fresh solution of PC. No further addition of L-serine was required. The 3rd and the 4th cycles were left under stirring at 40 °C for 30 h and 48 h respectively to obtain the major conversion of the substrate into PS. For each cycle, the final product was recovered in a mass yield of 85 %. ^{1}H NMR (spectrum reported in Figure S10): 0.75–0.86 (m, 6H, CH_3), 1.17–1.37 (m, 28H, CH_2 acyl chains), 1.49–1.63 (m, 4H, $\underline{CH_2}$-CH_2-COO), 1.89–2.04 (m, 6H, $\underline{CH_2}$-CH=CH), 2.18–2.28 (m, 4H, $\underline{CH_2}$-COO), 2.63–2.77 (m, 3H, CH=CH-$\underline{CH_2}$-CH=CH), 3.14–3.19 (CH_3-N-CH_2 residual PC), 3.51–3.62 (m, 1H, CH_2-$\underline{CH}$-NH_2), 3.77–3.97 (m, 4H, $\underline{OCH_2}$-CH-$\underline{CH_2}$-OPO_3), 4.05–4.14 (m, 1H, OPO_3-$\underline{CH_2}$), 4.30–4.40 (m, 1H, OPO_3-$\underline{CH_2}$),5.12–5.22(m, 1H, OCH_2-CHO-$\underline{CH_2}$-OPO_3), 5.23–5.40 (m, 6H, CH=CH). ESI/MS negative ion spectrum (reported in Figure S5): m/z 16:0/18:2-PS $[758.4]^-$, 18:2/18:2-PS $[782.4]^-$. ^{31}P NMR δ: −0.05 ppm.

Enzymatic preparation of phosphatidylethanolamine (PE)

30 mg of lyophilized PLD (0.026 U/mg) were dissolved in 1 mL of 0.1 M sodium acetate buffer pH 5.6 and 0.1 M of calcium chloride, and added dropwise to 5 mL of c-HLNPs (5 g/L). After 2 h, 2 M ethanolamine was added and the solution brought to pH 5.6 by addition of acetic acid. The solution was added to PC (10 mg) preliminary dissolved in 1 mL of toluene. The reaction was left under stirring at 40 °C for 24 h. Then the two phases were separated by centrifugation at 8000 rpm 2 min, and the aqueous phase was extracted with toluene (2×5 mL). The organic phases were collected, dried with sodium sulfate and the solvent was evaporated under reduced pressure. The PLD-c-HLNPs system was collected and recycled for 4 cycles, adding for each of them fresh PC. No addition of ethanolamine was required. The 3rd and the 4th cycles were left under stirring at 40 °C for 30 h and 48 h respectively to obtain the major conversion of the substrate into PE. For each cycle, the product was recovered in a mass yield of 50–60 %. ^{1}H NMR (spectrum reported in Figure S11): 0.79–0.90 (m, 6H, CH_3), 1.15–1.37 (m, 30 H, CH_2 acyl chains), 1.49–1.63 (m, 4H, $\underline{CH_2}$-CH_2-COO), 1.97–2.06 (m, 5 H, $\underline{CH_2}$-CH=CH), 2.20–2.34 (m, 4H, $\underline{CH_2}$-COO), 2.68–2.82 (m, 2H, CH=CH-$\underline{CH_2}$-CH=CH), 3.70–4.09 (m, 6H, $\underline{OCH_2}$-CH-$\underline{CH_2}$-OPO_3 and O-CH_2-$\underline{CH_2}$- NH_2), 4.09–4.17 (m, 1H, OPO_3-$\underline{CH_2}$), 4.30–4.40 (m, 1H, OPO_3-$\underline{CH_2}$), 5.15–5.24 (m, 1H, OCH_2-$\underline{CH}$-CH_2-OPO_3), 5.24–5.41 (m, 5H, CH=CH). ESI/MS spectra (reported in Figure S6): m/z 16:0/18:2-PE $[716.6]^+$, 18:2/18:2-PE $[740.7]^+$, 16:0/18:2- PE $[714.6]^-$, 18:2/18:2-PE $[738.6]^-$. ^{31}P NMR δ: 0.02 ppm.

Supporting Information

The following files are available free of charge:

Figure S1: Reaction of lignin hydroxymethylation and its side reactions; Figure S2: ^{31}P NMR of lignin and HL; Figure S3: ESI/MS of PC; Figure S4–S6: ESI/MS of the four recycling steps in PG, PS and PE synthesis; Figure S7: Scheme of preparation of PLD_B, PLD_D and PLD_{DL}; Figure S8: TLC of the main products; Figure S9–S11: ^{1}H NMR of PG, PS and PE. Tables S1–S4: Green metrics of the enzymatic transformations.

Author Contributions

LAMR: Investigation, Methodology, Visualization, Writing - Original Draft and Writing - Review and Editing. MHS: Funding acquisition; Conceptualization, Supervision and Writing - Review and Editing. PD: Funding acquisition; Conceptualization, Supervision and Writing - Review and Editing. MM: Methodology, Investigation, Visualization and Writing - Review and Editing. SS: Methodology, Investigation and Writing - Review and Editing. ER and PB: Investigation.

Acknowledgements

The authors gratefully acknowledge Walter Panzeri (SCITEC-CNR, Milano, Italy) for his technical support on ESI/MS analysis. M.H.S. acknowledges funding from Vetenskapsrådet (grant number 2020-03752) and Vinnova (grant number 2019-03174). P.D. acknowledges the two projects financed by PNRR MUR and NextGenerationEU: "ONFOODS-Research and innovation network on food and nutrition Sustainability, Safety and Security" (grant number PE0000003), and "National Research Centre for Agricultural Technologies-AGRITECH" (grant number CN00000022). L.A.M.R. acknowledges MUR for PhD grant (XXXVI Research Doctorate Cycle). The authors acknowledge funding from the Knut and Alice Wallenberg Foundation (KAW) through the Wallenberg Wood Science Center (grant number KAW 2021.0313).

Conflict of Interests

The authors declare no conflict of interest.

Data Availability Statement

The data that support the findings of this study are available from the corresponding author upon reasonable request.

Keywords: Lignin nanoparticles · phospholipids · biocatalysis · phospholipase D · sustainability · circular economy

[1] a) S. Drescher, P. van Hoogevest, *Pharmaceutica* **2020**, *12*, 1235; b) B. Wang, P. Tontonoz, *Annu. Rev. Physiol.* **2019**, *81*, 165–188; c) M. Falconi, S. Ciccone, P. D'Arrigo, F. Viani, R. Sorge, G. Novelli, P. Patrizi, A. Desideri, S. Biocca, *Biochem. Biophys. Res. Commun.* **2013**, *438*, 340–345; d) R. Ventura, I. Martínez-Ruiz, M. I. Hernández-Alvarez, *Biomedicine* **2022**, *10*, 1201; e) M. K. Ahmmed, F. Ahmmed, H. Tian, A. Carne, A. E.-D. Bekhit, *Compr. Rev. Food Sci. Food Saf.* **2020**, *19*, 64–123; f) F. Baldassarre, C. Allegretti, D. Tessaro, E. Carata, C. Citti, V. Vergaro, C. Nobile, G. Cannazza, P. D'Arrigo, A. Mele, L. Dini, G. Ciccarella, *ChemistrySelect* **2016**, *1*, 6507–6514.

[2] P. D'Arrigo, M. Scotti, *Curr. Org. Chem.* **2013**, *17*, 812–830.
[3] a) D. Küllenberg, L. A. Taylor, M. Schneider, U. Massing, *Lipids Health Dis.* **2012**, *11*, 3; b) C.-C. Wang, L. Du, H.-H. Shi, L. Ding, T. Yanagita, C.-H. Xue, Y.-M. Wang, T.-T. Zhang, *Mol. Nutr. Food Res.* **2021**, *65*, 2100009.
[4] J. Li, Y. He, S. Anankanbil, Z. Guo, in *Biobased Surfactants (Second Edition)* (Eds.: D. G. Hayes, D. K. Y. Solaiman, R. D. Ashby), AOCS Press, **2019**, pp. 243–286.
[5] a) P. Liu, G. Chen, J. Zhang, *Molecules* **2022**, *27*, 1372; b) B. N. Aldosari, I. M. Alfagih, A. S. Almurshedi, *Pharmaceutica* **2021**, *13*, 206.
[6] P. D'Arrigo, C. Giordano, P. Macchi, L. Malpezzi, G. Pedrocchi-Fantoni, S. Servi, *The International Journal of Artificial Organs* **2007**, *30*, 133–143.
[7] a) U. Massing, H. Eibl, *Chem. Phys. Lipids* **1995**, *76*, 211–224; b) E. Fasoli, A. Arnone, A. Caligiuri, P. D'Arrigo, L. de Ferra, S. Servi, *Org. Biomol. Chem.* **2006**, *4*, 2974–2978; c) P. D'Arrigo, E. Fasoli, G. Pedrocchi-Fantoni, C. Rossi, C. Saraceno, D. Tessaro, S. Servi, *Chem. Phys. Lipids* **2007**, *147*, 113–118.
[8] a) P. D'Arrigo, L. de Ferra, G. Pedrocchi-Fantoni, D. Scarcelli, S. Servi, A. Strini, *J. Chem. Soc. Perkin Trans. 1* **1996**, 2657–2660, https://doi.org/10.1039/P19960002657; b) L. R. Juneja, N. Hibi, N. Inagaki, T. Yamane, S. Shimizu, *Enzyme Microb. Technol.* **1987**, *9*, 350–354; c) Z. J. Struzik, S. Biyani, T. Grotzer, J. Storch, D. H. Thompson, *Molecules* **2022**, *27*, 2199.
[9] P. D'Arrigo, S. Servi, *Trends Biotechnol.* **1997**, *15*, 90–96.
[10] a) C. Allegretti, F. Denuccio, L. Rossato, P. D'Arrigo, *Catalysts* **2020**, *10*, 997; b) C. Allegretti, F. G. Gatti, S. Marzorati, L. A. M. Rossato, S. Serra, A. Strini, P. D'Arrigo, *Catalysts* **2021**, *11*, 655; c) G. Carrea, P. D'Arrigo, F. Secundo, S. Servi, *Biotechnol. Lett.* **1997**, *19*, 1083–1085.
[11] P. D'Arrigo, L. Cerioli, C. Chiappe, W. Panzeri, D. Tessaro, A. Mele, *J. Mol. Catal. B* **2012**, *84*, 132–135.
[12] a) Z.-Q. Duan, F. Hu, *Green Chem.* **2012**, *14*, 1581–1583; b) W. Qin, C. Wu, W. Song, X. Chen, J. Liu, Q. Luo, L. Liu, *Process Biochem.* **2018**, *66*, 146–149; c) Y. H. Bi, Z. Q. Duan, W. Y. Du, Z. Y. Wang, *Biotechnol. Lett.* **2015**, *37*, 115–119.
[13] J. Bié, B. Sepodes, P. C. B. Fernandes, M. H. L. Ribeiro, *Processes* **2022**, *10*, 494.
[14] N. G. Lewis, E. Yamamoto, *Annu. Rev. Plant Physiol. Plant Mol. Biol.* **1990**, *41*, 455–496.
[15] a) D. S. Bajwa, G. Pourhashem, A. H. Ullah, S. G. Bajwa, *Ind. Crops Prod.* **2019**, *139*, 111526; b) S. Bertella, J. S. Luterbacher, *Trends Chem.* **2020**, *2*, 440–453; c) A. Ekielski, P. K. Mishra, *Int. J. Mol. Sci.* **2021**, *22*, 63; d) T. I. Korányi, B. Fridrich, A. Pineda, K. Barta, *Molecules* **2020**, *25*, 2815; e) X. Wu, M. V. Galkin, T. Stern, Z. Sun, K. Barta, *Nat. Commun.* **2022**, *13*, 3376.
[16] a) V. K. Yadav, N. Gupta, P. Kumar, M. G. Dashti, V. Tirth, S. H. Khan, K. K. Yadav, S. Islam, N. Choudhary, A. Algahtani, S. P. Bera, D. H. Kim, B. H. Jeon, *Materials (Basel)* **2022**, *15*, 953; b) A. Moreno, J. Liu, M. Morsali, M. H. Sipponen, in *Micro and Nanolignin in Aqueous Dispersions and Polymers* (Eds.: D. Puglia, C. Santulli, F. Sarasini), Elsevier, **2022**, pp. 385–431.
[17] a) M. Ma, L. Dai, J. Xu, Z. Liu, Y. Ni, *Green Chem.* **2020**, *22*, 2011–2017; b) S. Iravani, R. S. Varma, *Green Chem.* **2020**, *22*, 612–636; c) W. Zhao, B. Simmons, S. Singh, A. Ragauskas, G. Cheng, *Green Chem.* **2016**, *18*, 5693–5700; d) T. Pang, G. Wang, H. Sun, L. Wang, Q. Liu, W. Sui, A. M. Parvez, C. Si, *ACS Sustainable Chem. Eng.* **2020**, *8*, 9174–9183.
[18] a) M. B. Agustin, P. A. Penttilä, M. Lahtinen, K. S. Mikkonen, *ACS Sustainable Chem. Eng.* **2019**, *7*, 19925–19934; b) F. A. Petrie, J. M. Gorham, R. T. Busch, S. O. Leontsev, E. E. Urena-Benavides, E. S. Vasquez, *Int. J. Biol. Macromol.* **2021**, *181*, 313–321; c) I. Pylypchuk, M. H. Sipponen, *Green Chem.* **2022**, *24*, 8705–8715.
[19] S. Beisl, J. Adamcyk, A. Friedl, *Molecules* **2020**, *25*, 1388.
[20] C. H. M. Camargos, C. A. Rezende, *Int. J. Biol. Macromol.* **2021**, *193*, 647–660.
[21] a) A. Tribot, G. Amer, M. A. Alio, H. De Baynast, C. Delattre, A. Pons, J.-D. Mathias, J.-M. Callois, C. Vial, P. Michaud, *Eur. Polym. J.* **2019**, *112*, 228–240; b) M. Lievonen, J. J. Valle-Delgado, M.-L. Mattinen, E.-L. Hult, K. Lintinen, M. A. Kostiainen, A. Paananen, G. R. Szilvay, H. Setälä, M. Österberg, *Green Chem.* **2016**, *18*, 1416–1422.
[22] A. Henn, M. L. Mattinen, *World J. Microbiol. Biotechnol.* **2019**, *35*, 125.
[23] W. D. H. Schneider, A. J. P. Dillon, M. Camassola, *Biotechnol. Adv.* **2021**, *47*, 107685.
[24] E. Capecchi, D. Piccinino, I. Delfino, P. Bollella, R. Antiochia, R. Saladino, *Nanomaterials (Basel)* **2018**, *8*, 438.
[25] a) Z. Zhang, V. Terrasson, E. Guenin, *Nanomaterials (Basel)* **2021**, *11*, 1336; b) F. T. T. Cavalcante, A. L. G. Cavalcante, I. G. de Sousa, F. S. Neto, J. C. S. dos Santos, *Catalysts* **2021**, *11*, 1222; c) M. Bilal, M. Asgher, H. Cheng, Y. Yan, H. M. N. Iqbal, *Crit. Rev. Biotechnol.* **2019**, *39*, 202–219.
[26] a) K. S. Muthuvelu, R. Rajarathinam, R. N. Selvaraj, V. B. Rajendren, *Int. J. Biol. Macromol.* **2020**, *152*, 1098–1107; b) D. Piccinino, E. Capecchi, L. Botta, P. Bollella, R. Antiochia, M. Crucianelli, R. Saladino, *Catalysis Science, Technology* **2019**, *9*, 4125–4134; c) E. Capecchi, D. Piccinino, E. Tomaino, B. M. Bizzarri, F. Polli, R. Antiochia, F. Mazzei, R. Saladino, *RSC Adv.* **2020**, *10*, 29031–29042; d) A. Moreno, M. H. Sipponen, *Nat. Commun.* **2020**, *11*, 5599.
[27] S. Mao, Z. Zhang, X. Ma, H. Tian, F. Lu, Y. Liu, *Int. J. Biol. Macromol.* **2021**, *169*, 282–289.
[28] Q. Han, H. Zhang, J. Sun, Z. Liu, W.-c. Huang, C. Xue, X. Mao, *Catalysts* **2019**, *9*, 361.
[29] Y. Zhang, L. Zhu, G. Wu, X. Wang, Q. Jin, X. Qi, H. Zhang, *Colloids Surf. B* **2021**, *202*, 111668.
[30] S. Furse, *Journal of Chemical Biology* **2017**, *10*, 1–9.
[31] a) H. Y. Kim, B. X. Huang, A. A. Spector, *Prog. Lipid Res.* **2014**, *56*, 1–18; b) M. J. Glade, K. Smith, *Nutrition (Burbank, Los Angeles County, Calif.)* **2015**, *31*, 781–786.
[32] a) E. Calzada, O. Onguka, S. M. Claypool, in *International Review of Cell and Molecular Biology, Vol. 321* (Ed.: K. W. Jeon), Academic Press, **2016**, pp. 29–88; b) D. Patel, S. N. Witt, *Oxidative Medicine and Cellular Longevity* **2017**, *2017*, 4829180.
[33] L. Cui, D. J. McClements, E. A. Decker, *J. Agric. Food Chem.* **2015**, *63*, 3288–3294.
[34] C. Allegretti, S. Fontanay, K. Rischka, A. Strini, J. Troquet, S. Turri, G. Griffini, P. D'Arrigo, *ACS Omega* **2019**, *4*, 4615–4626.
[35] a) H. Paananen, L. Alvila, T. T. Pakkanen, *Sustainable Chemistry and Pharmacy* **2021**, *20*, 100376; b) I. A. Gilca, R. E. Ghitescu, A. C. Puitel, V. I. Popa, *Iran. Polym. J.* **2014**, *23*, 355–363.
[36] a) T. Măluţan, R. Nicu, V. I. Popa, *BioResources* **2008**, *3*, 13–20;b) O. Faix, *Holzforschung* **1991**, *45*, 21–28.
[37] a) I. V. Pylypchuk, A. Riazanova, M. E. Lindström, O. Sevastyanova, *Green Chem.* **2021**, *23*, 3061–3072; b) M. Morsali, A. Moreno, A. Loukovitou, I. Pylypchuk, M. H. Sipponen, *Biomacromolecules* **2022**, *23*, 4597–4606.
[38] X. Zhao, M. Guo, X. Li, B. Liu, B. Li, J. Wang, *Appl. Biochem. Biotechnol.* **2023**, 1–13.
[39] C. Allegretti, A. Bono, P. D'Arrigo, F. G. Gatti, S. Marzorati, L. A. M. Rossato, S. Serra, A. Strini, D. Tessaro, *ChemistrySelect* **2021**, *6*, 9157–9163.
[40] B. Li, J. Wang, X. Zhang, B. Zhao, *Ind. Eng. Chem. Res.* **2016**, *55*, 10555–10565.
[41] Y. Li, J.-Q. Wu, N.-B. Long, R.-F. Zhang, *Int. J. Biol. Macromol.* **2019**, *141*, 60–67.
[42] C. Allegretti, A. Bono, P. D'Arrigo, F. G. Gatti, S. Marzorati, L. A. Rossato, S. Serra, A. Strini, D. Tessaro, *ChemistrySelect* **2021**, *6*, 9157–9163.
[43] P. T. Anastas, J. C. Warner, *Frontiers* **1998**, *640*, 850.
[44] X. Meng, C. Crestini, H. Ben, N. Hao, Y. Pu, A. J. Ragauskas, D. S. Argyropoulos, *Nat. Protoc.* **2019**, *14*, 2627–2647.
[45] S. Imamura, Y. Horiuti, *The Journal of Biochemistry* **1978**, *83*, 677–680.

Manuscript received: June 7, 2023
Revised manuscript received: September 8, 2023
Accepted manuscript online: October 6, 2023
Version of record online: November 14, 2023